Heliyon 10 (2024) e28308

Contents lists available at ScienceDirect

Heliyon

journal homepage: www.cell.com/heliyon

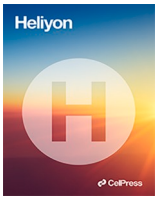

Research article

Phase transformation sequence of pre-oxidized roast-leach ferrovanadium residue

M. Nevondo [a,*], L. Koech [a], O.O. Ola-omole [b,c], M.M. Ramakokovhu [a], M.L. Teffo [a], R. Sadiku [a]

[a] *Institute for NanoEngineering Research, Department of Chemical, Metallurgical and Materials Engineering, Tshwane University of Technology, Pretoria, 0001, South Africa*
[b] *School of Mining, Metallurgy and Chemical Engineering, University of Johannesburg, Johannesburg, 2000, South Africa*
[c] *Metallurgical and Materials Engineering Department, Federal University of Technology, Akure, Nigeria*

ARTICLE INFO

Keywords:
Mineralogy
Phase transformation sequence
Pre-oxidation
Titanomagnetite

ABSTRACT

The depletion of the primary metal sources has prompted the exploration of alternative avenues for metal recovery. In the case of titanium and iron, the ferrovanadium residue produced through roast-leach processing of titanomagnetite presents a viable option for accessing these metals. Titanomagnetite resources, which contain valuable elements, such as iron, vanadium, and titanium, possess significant valuable potential. Titanomagnetite deposits are normally treated via smelting for vanadium or vanadium and iron recovery; titanium is not commercially recoverable. Titanomagnetites have recently been processed through the roast-leach method for vanadium primary production, and iron and titanium are typically part of the waste stream in this process. This study proposes a novel approach to determine the characteristic mineralogy and to study the phase transformation sequence of the roasted-leached ferrovanadium residue during the pre-oxidation process. Leaching was also done to evaluate the extraction potential of Fe, V and Ti on the pre-oxidized residue in comparison to the raw residue The roasted-leached ferrovanadium residue was sampled using the cone and quartering method and then, dried in an oven at temperatures of between 30 and 40 °C, for an hour after which, the remaining moisture content was determined. The bond milling method was employed to reduce the sample size, while the particle size distribution (PSD) was verified by using the standard laboratory Tyler series. Thereafter, the roasted-leached ferrovanadium residue was characterized with XRD, SEM, ICP-OES, and XRF. The samples were pre-oxidized at temperatures ranging from 300 °C to 1000 °C with an aim of improving the grades of iron, vanadium, and titanium-bearing minerals prior leaching. The results revealed the moisture content to be ~5.07%. The bond work index of typical slags was estimated to be 10.2 kwh/t, with a determined d_{80} value of 200 μm. According to the XRF analysis, the predominant compounds present are hematite, Fe_2O_3 (75.55%), titanium dioxide, TiO_2 (12.79%), silicon dioxide, SiO_2 (3.03%), and alumina, Al_2O_3 (2.62%), along with minor compounds. XRD patterns exhibited the presence of $FeTiO_3$ and VO_2 in the as-received samples, while pre-oxidation induced the evolution of new phases such as hematite, rutile, anatase, and pseudobrookite.

* Corresponding author.
E-mail address: mbavhanevondo@gmail.com (M. Nevondo).

https://doi.org/10.1016/j.heliyon.2024.e28308
Received 29 October 2023; Received in revised form 15 March 2024; Accepted 15 March 2024
Available online 16 March 2024

1. Introduction

Vanadiferous titaniferous magnetite deposits also known as titanomagnetites deposits with vanadium occurring in the magnetite are located in the Bushveld Complex of South Africa [1,2]. Titanomagnetite resources which contain valuable elements such as: iron, vanadium, and titanium, possess significant valuable potentials [3–5]. Consequently, the exploitation of titanomagnetite has attracted considerable attention [6–8]. Vanadium is contained in titanomagnetite to a significant extent (between 1.2 and 2.2% V_2O_5), and it has been historically mined by various companies. Titanomagnetites also contain iron ore in the form of magnetite and titanium with concentrations ranging between 50 and 75% of FeO to between 12 and 21% of TiO_2. Titaniferous ores have traditionally been dismissed as a source of iron and titanium; this is due to the known difficulties of using iron ore with high titania content in a blast furnace operation [9].

Titanomagnetite serves as a primary source of vanadium, with approximately 88% of the world's vanadium being extracted from this mineral [9,10]. Traditionally, the blast furnace and basic oxygen furnace processes have been employed for vanadium and iron recovery in titanomagnetite utilization. However, these processes exhibit relatively low recovery ratios for iron (in pig iron), vanadium (in vanadium slag), and titanium (in ilmenite). Moreover, a significant amount of high-titanium slag is discarded resulting in the resource wastage and the associated environmental pollution [11]. Various alternative processes including chemical extraction, direct reduction, and electric arc furnace (EAF) smelting procedures have been proposed and studied. However, most of these processes have not demonstrated commercial viability due to poor selectivity, low recovery rates, and limited economic efficiency [12,13]. Moreover, due to their low grades, fine grain size, and complex mineralogy, titanomagnetite ores pose challenges in their treatment [1,2].

Recently, titanomagnetites are also processed through the roast-leach process for vanadium primary production. However, in this process, iron and titanium generally form part of the waste stream [14]. The conventional roast-leach process involves roasting vanadium-bearing titanomagnetite in the presence of a sodium reagent (e.g., salt (NaCl), sodium sulphate (Na_2SO_4), and soda ash (Na_2CO_3) as common sodium sources), followed by controlled pH leaching with water as the lixiviant. This method effectively rejects impurities, yielding sodium metavanadate ($NaVO_3$) [15]. The aim of the roasting stage is to convert vanadium species in titanomagnetite into leachable phases [16]. The roast-leach process is deemed superior to the smelting process in terms of cumulative vanadium recovery [17].

The processing of ferrovanadium through the roast-leach process results in the generation of significant quantities of waste slag stockpiles derived from titanomagnetite. These stockpiles typically, consist of titanium (in the form of rutile) and highly magnetic iron hence, rendering them unusable. However, the comprehensive utilization of these tailings has gained increasing importance due to the stricter environmental regulations, cleaner production standards, and the scarcity of valuable resources [18,19].

Thermogravimetric analysis or thermal gravimetric analysis (TGA) is a method of thermal analysis in which the mass of a sample is measured over time as the temperature changes. TGA aids in the identification of phase transformations prior pre-oxidation. Pre-oxidation, also referred to as calcination, involves subjecting the sample to heat in the presence of oxygen in order to observe the sequence of phase transformations during this process [20]. Ramakokovhu et al. [20] examined the characteristics of the pre-oxidized metastable ilmenite phases by using the electrochemical techniques to acquire thermodynamic data. The thermodynamic data indicated the specific temperatures at which phase transformation occurs by using the enthalpy heat of fusion characterization technique. This phase quantification of the thermodynamic data enables an opportunity to target the optimum temperature and obtain the desired phases prior to subsequent purification process. The results revealed that at 816 °C, ilmenite decomposed to form a new solid-solid intermediate metastable phase, $Fe_3Ti_2O_7$ (pseudorutile), which is amenable to leaching.

This study seeks to determine the characteristic mineralogy of the roast-leach ferrovanadium residue and investigates the phase transformation sequence experienced during pre-oxidation. An acid-leaching process was also utilized to determine the extraction potential of iron, vanadium, and titanium from both the raw residue and the pre-oxidized residue. The roast-leach ferrovanadium residue was subjected to mineralogical characterization by using the integrated instrumental techniques to obtain detailed information on the phases and phase transformation, morphology and chemical composition of the as-received and pre-oxidized roast-leach ferrovanadium residue. The intention is to comprehensively utilize the roast-leach ferrovanadium residue by recovering Fe, V, and Ti and the resulting residue will be environmentally benign and suitable for use as construction materials [12,13]. This could be the potential solution for reducing environmental pollution and improving the economic sustainability of minerals [21].

2. Methodology

2.1. Sample sourcing and preparation

The residue used in this study was obtained from the Main Magnetite Layer (MML) of the Bushveld Complex in South Africa, following the roast-leach processing to produce ferrovanadium and waste residue. The sample was prepared by an initial sampling procedure using cone and quartering method and then dried in an oven at a temperature between 30 and 40 °C for 1 h to remove moisture. The as-received roast-leach ferrovanadium residue went through size reduction using a ball mill and a pulverizer to achieve 80% of the pulverized sample passing through a 75-μm sieve. To determine the appropriate number of balls for the ball mill, a ratio of 1:4 was employed, where one represented the mass of the ball and four represented the mass of the sample. Accordingly, the necessary weight of the balls was recorded, and milling was conducted for a duration of 1 h. After milling, a rotary splitter was utilized to obtain a representative sample. Sample bags, laboratory scale, and a sample scoop were employed in the preparation and collection of the required samples. As part of sample preparation, the moisture content of the residue was determined. The particle size distribution of the sample was determined through sieve analysis, a technique involving the sifting of the sample through a stack of wire mesh sieves

to separate it into distinct size ranges. To facilitate this process, a sieve shaker was utilized to vibrate the sieve stack for a specific duration of 30 min. The vibration facilitated the re-orientation of particles with irregular shapes as they passed through the sieves. The resulting particle size distribution was then determined and verified by using the standard laboratory Tyler series sieves, as both methods provided information on the cut size.

The TGA was employed to investigate the behaviour of phase changes in both the as-received roast-leach residue and the raw ilmenite. This measurement provides information about various physical phenomena, such as phase transitions, absorption, adsorption, and desorption, as well as possible chemical phenomena like chemisorption, thermal decomposition and solid-gas reactions (e.g., oxidation or reduction). The TGA played a crucial role in identifying the phase transformations that occurred prior to pre-oxidation procedure.

2.2. Pre-oxidation of the roast-leach ferrovanadium residue

The pre-oxidation process of the roast-leach ferrovanadium residue was conducted in a muffle furnace at temperatures ranging from 300° to 1000 °C for durations of between 30 min and 3 h. An electrical-resistance-heated muffle furnace was utilized, with crucibles serving as heating vessels within the furnace. The furnace ramping speed rate was set at 10 °C per minute. At every 30 min interval, the pre-oxidized roast-leach ferrovanadium residue was taken out of the furnace and the mineralogical characteristics of the pre-oxidized roast-leach ferrovanadium residue was determined. The phase transformations that occurred during pre-oxidation process are outlined in equations (1)–(3) below:

$$4FeTiO_{3(s)} + O_{2(g)} \rightarrow 2Fe_2O_{3(s)} + 4TiO_{2(s)} \quad (1)$$

$$4FeTiO_{3(s)} + O_{2(g)} \rightarrow 2Fe_2TiO_{5(s)} + 2TiO_{2(s)} \quad (2)$$

$$TiO_{2(s)} + Fe_2O_{3(s)} \rightarrow Fe_2TiO_{5(s)} \quad (3)$$

2.3. Mineralogical analysis

The roast-leach ferrovanadium residue and the pre-oxidized residue went through a comprehensive characterization process utilizing integrated instrumental techniques to obtain detailed information as outlined by Samal et al., [22]. After milling and sizing of the residue, wet and dry chemical analyses were conducted. The phase identification studies of the samples were conducted using XRD technique. The samples were examined by using a PANalytical X'Pert Pro powder diffractometer, equipped with an X'Celerator detector and variable divergence and receiving slits with Fe-filtered Co-K_α radiation. The X'Pert High score plus software was used to identify the phases. The chemical composition of the samples was determined by using ZSX Primus II XRF machine. The morphological structure of the samples was examined using the JEOL, JSM-7600F. The machine was operated with a 20 KV voltage and a working distance of 15 mm was set between the specimen and the detector. The solutions obtained after the aqua regia digestion, were analyzed by using the ICP-OES to perform the compositional analysis. The Fe, V, and Ti concentrations were determined by using a Spectro ARCOS® ICP-OES.

3. Results and discussions

3.1. Characterization of the as-received roast-leach ferrovanadium residue

3.1.1. Physical properties and size reduction results

The moisture content of the as-received roast-leach ferrovanadium residue was determined to be 5.07%, falling within an

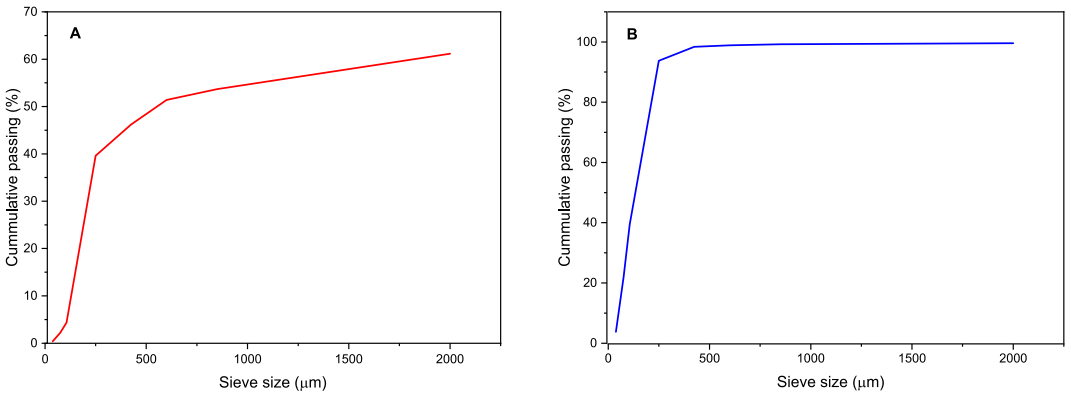

Fig. 1. Particle size distribution curve of as-received roast-leach ferrovanadium residue (A) before milling and (B) after milling.

acceptable range that does not require extensive drying. This moisture level enables easy handling during PSD analysis, as excessive moisture content can potentially result in sample agglomeration. The bond work index for typical slags was estimated at 10.2 kWh/t by Michaud [23] resulting in a calculated work/energy input of 7.35 kWh/t. A higher bond work index value indicates increased difficulty in grinding the material. According to Michaud [23] and Mkurazhizha [24], residue (slag) is classified as having medium hardness based on the work index. Minerals are categorized by their work index into extremely hard (19.81–30.99), hard (13.37–16.76), medium (8.01–10.33), and soft (4.73–6.22). With a bond work index falling within the medium hardness range, grinding this material should not present significant challenges.

Fig. 1**(A)** presents the particle size distribution of the as-received roast-leach ferrovanadium residue, determined by the laboratory Tyler series. The results indicate that the particle size of 500 μm had a 50% passing rate, denoted as d_{50}. However, the particle size corresponding to the 80% passing rate, known as d80, could not be detected in this experimental procedure. This absence of d_{80} suggests that the material is quite coarse, necessitating milling to achieve sample liberation. Fig. 1(B) also shows the particle size distribution of the roast-leach ferrovanadium residue after milling. The results indicate that the majority of the particle sizes (d_{80}) were found within a range of −200 μm and +106 μm, signifying some degree of liberation during milling. Thus, in this study, a pulverizer was used for further size reduction to achieve the 80% passing of 75 μm.

3.1.2. Mineralogical analysis of the as-received roast-leach ferrovanadium residue

The chemical composition of the raw roast-leach ferrovanadium residue, analyzed by using the XRF, is presented in Table 1. Hematite (Fe_2O_3) is the dominant mineral, comprising 75.55% of the residue's weight. Titanium dioxide (TiO_2) at 12.79% is the next significant component. Titanium dioxide is commonly associated with minerals, such as ilmenite, rutile, and anatase [25]. Additionally, the residue contains 3.03% silica (SiO_2) and 2.62% alumina. These findings highlight the presence of some undesirable compounds in the residue that will require removal during the reclamation process.

Table 2 presents the average concentrations of iron, titanium, and vanadium in the residue, as determined by ICP-OES. Each value in Table 2, represents the average of three trials. The highest concentrations of Fe and Ti were observed to be 63,789.00 mg/ℓ and 5339.00 mg/ℓ, respectively, at a particle size of 75 μm. Similarly, the highest concentration of vanadium was found to be 63.74 mg/ℓ at the same particle size. This indicates the fact that by reducing the particle size to 75 μm, is necessary to achieve the liberation of Fe, Ti, and V. These specific particle sizes represent the effective liberation sizes for each of the elements.

The X-ray diffraction (XRD) analysis of the residue particles at various sizes, ranging from 600 μm to −38 μm, and the raw sample, as shown in Fig. 2, reveals the presence of $FeTiO_3$ (ilmenite) and VO_2 (vanadium oxide). Ilmenite is the dominant crystalline phase, followed by vanadium oxide, indicating the typical composition found in metallurgical slags [3,26]. The presence of these valuable components in the residue, emphasizes the importance of reclaiming and recycling them to prevent environmental challenges. It is crucial for the metallurgical industry to explore methods of transforming these waste materials into valuable resources, and hence, promoting a zero-waste approach through recycling and reuse.

Fig. 3 **(A, B)** shows the SEM micrographs of the as-received roast-leach ferrovanadium residue. The results show that the microstructures contain particles of different shapes and sizes, small to medium and large particles with different shades and textures. The results show that ilmenite is associated with a light grey shade that is dominant, followed by a blackish or dark shade, associated with vanadium dioxide. The light grey shade has a considerable smoother texture than the blackish darker shade, which has a rough texture [27]. The variation in shades from light to dark grey, confirmed the association of titanomagnetite with other minerals [28].

3.1.3. Thermogravimetric analysis of the as-received roast-leach ferrovanadium residue versus ilmenite

The thermogravimetric properties of the as-received roast-leach ferrovanadium residue was compared with ilmenite, a metal oxide mineral that primarily consists of iron and titanium oxide ($FeTiO_3$). The rationale behind this comparison stems from the ilmenite's historical use as a key source of titanium metal. It was anticipated that the thermogravimetric analysis of the as-received roast-leach ferrovanadium residue used in this study, would exhibit a similar pattern to that of ilmenite. Hence, this comparison was undertaken to explore any resemblances or correlations between the two materials. Their phase transitions were examined under oxygen at temperatures ranging from 100 °C to 1000 °C. Fig. 4 illustrates the TGA results for ilmenite, while Fig. 5 presents the TGA results for the as-received roast-leach ferrovanadium residue. Both graphs display similar trends. In the TGA analysis of ilmenite, a phase change was observed at ~350 °C, followed by a prominent peak at ~816 °C, indicating significant phase transitions. Similarly, the TGA analysis of the as-received roast-leach ferrovanadium residue, showed a comparable pattern with a phase change occurring at ~350 °C and a significant peak observed at 816 °C. These findings highlight the similarity in the thermal behaviour of the two samples, during their TGA analyses. These findings align with the research conducted by Ramakokovhu et al. [29], which demonstrated that at 816 °C, ilmenite decomposed to form a new intermediate metastable phase known as a heterostructure of $Fe_2O_3{\cdot}2TiO_2$. The TGA analysis tally with the phase transformation interpretation from the XRD, XRF, and SEM analyses of the pre-oxidized roast-leach ferrovanadium residue. A similar pattern is observed with weight loss at 300 °C. The calculated weight loss was 0.39% for ilmenite and 0.43% for the roast leach residue. This indicates that the roast leach residue had a slightly higher weight loss compared to ilmenite.

Table 1
Chemical composition of the raw roast-leach ferrovanadium residue determined by XRF analysis.

Components (wt.%)							
Na_2O	MgO	Al_2O_3	SiO_2	CaO	TiO_2	Cr_2O_3	Fe_2O_3
1.85	0.22	2.62	3.03	0.59	12.79	0.11	75.55

Table 2
Results of ICP-OES the raw roast-leach ferrovanadium residue after aqua regia digestion.

Name of element	symbol	Average quantity (mg/l) at different particle sizes			
		38 μm	75 μm	105 μm	250 μm
Iron	**Fe**	62,362.00	63,789.00	62,312.00	62,311.00
Titanium	**Ti**	5230.00	5339.00	5225.00	5013.00
Vanadium	**V**	62.57	63.74	62.54	61.99

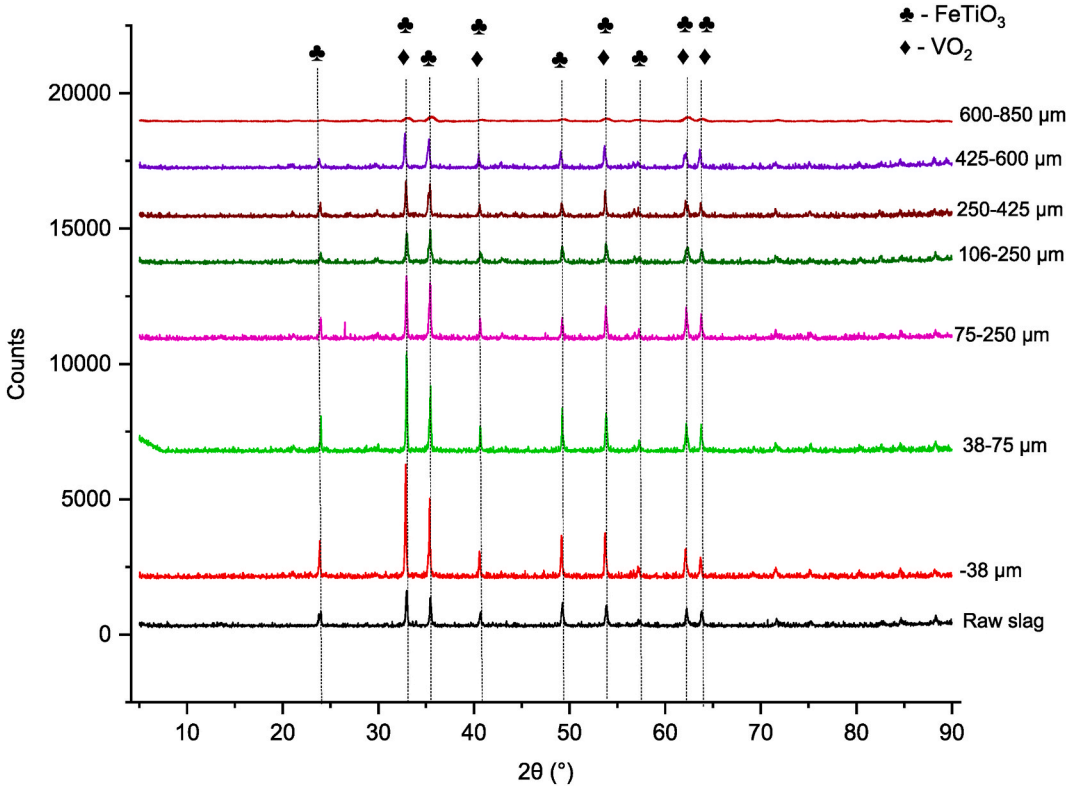

Fig. 2. XRD after milling at different particle sizes ranging from −38 to 850 μm.

3.2. Mineralogical analysis of the pre-oxidized roast-leach ferrovanadium residue

3.2.1. XRD analysis of pre-oxidized roast-leach ferrovanadium residue

XRD analysis was conducted to study the phase transformation of the residue during pre-oxidation. The residue underwent calcination in a furnace, utilizing the temperature parameters specified in the literature [29]. The temperature range spanned from 300 °C to 1000 °C, and samples were extracted at 30-min intervals over a total duration of 3 h. During the pre-oxidation process, notable changes were observed in the XRD patterns as exhibited in Fig. 6 (A-C), indicating the emergence of new peaks at various temperatures and durations of the pre-oxidation process. These findings suggest the presence of compounds other than ilmenite and vanadium dioxide [30] aligning with the schematized reactions in section 2.2 (equations (1)–(3)). Specifically, the peaks corresponding to ilmenite and hematite were detected at the diffraction peaks of 25°, 34°, and 36° [31]. These phases were detected as dominant phases in the raw slag as evident in Fig. 6(A). Subsequently, the crystalline phases of hematite, pseudobrookite, rutile, and anatase emerged [17] as observed at 500 °C, for 2 h. Similarly, at 600 °C for 3 h and 700 °C for 2½ hours, the same phases were present, with an increased occurrence of rutile and hematite at 700–800 °C and pseudobrookite at above 900 °C, as also observed in the XRD quantitative analysis in Table 3. Distortions in the crystal lattice were observed at temperatures of between 900 °C and 1000 °C, accompanied by diminishing hematite, rutile and ilmenite phases. According to Equation (2), the transformation of ilmenite into pseudobrookite accounts for the reduction in ilmenite phases observed after reaching 900 °C. Simultaneously, as per Equation (3), hematite and rutile undergo consumption, leading to their decline beyond 900 °C. These observations are further validated by the quantitative XRD analysis presented in Table 3. However, studies on the pre-oxidation of ilmenite, have confirmed the formation of another phase, $Fe_3Ti_3O_9$ (pseudorutile), at a temperature of ~814 °C [32]. This pseudorutile phase is known to be amenable to leaching. This phase was not detected in the pre-oxidized residue samples examined in this study.

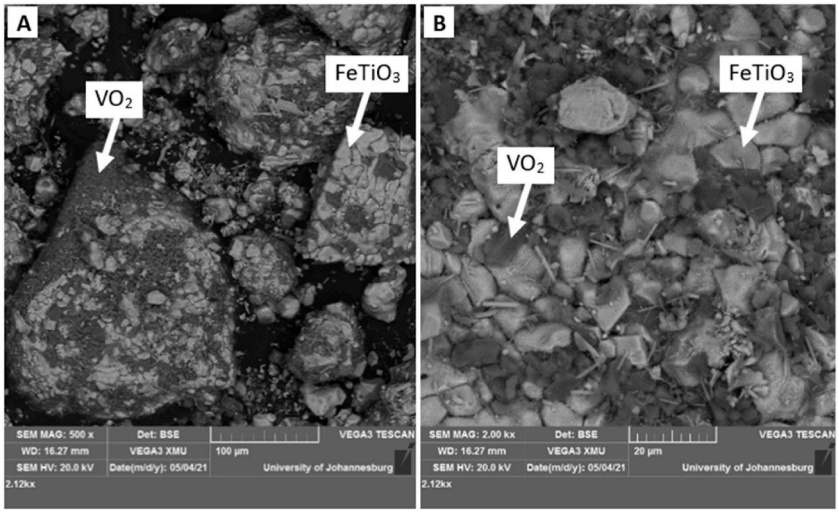

Fig. 3. SEM microstructure image of the as-received roast-leach ferrovanadium residue under different magnifications (A) 100 μm and (B) 20 μm.

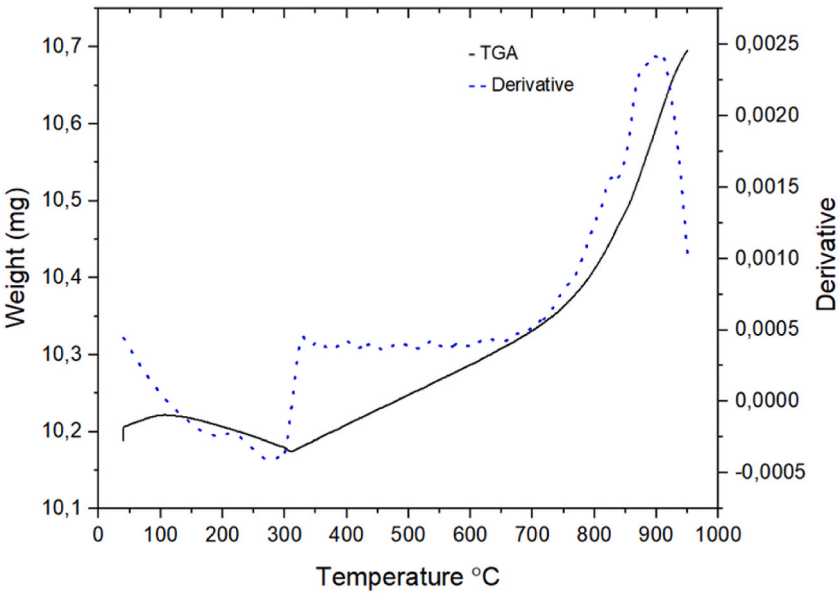

Fig. 4. Thermogravimetric analysis of ilmenite.

3.2.2. XRF analysis of pre-oxidized roast-leach ferrovanadium residue

The results from the XRF in Table 4, show the chemical composition of the pre-oxidized roast-leach ferrovanadium residue at 700 °C, 800 °C and 900 °C. At 800 °C, minimal variations were observed, with a slightly higher rutile formation of 14.01% and Fe_2O_3 content of 77.52% when compared to the residue that were pre-oxidized at 700 °C and 900 °C. These findings align with the XRD results, indicating an increased formation of the rutile phase and Fe_2O_3 at 800 °C and confirming the occurrence of phase transformation during pre-oxidation. At 900 °C, there was a minimal rutile formation of ~13.56% and Fe_2O_3 content of ~76.91%. These results align with a study by Ramakokovhu et al. [29], suggesting that at temperatures above 900 °C, the rutile hematite and rutile phases forms another phase, known as pseudobrookite.

The significant iron (Fe) content is attributed to the abundant presence of ilmenite, as evidenced from the XRD results. On the other hand, the presence of silicon (Si) is attributed to the occurrence of the quartz phases. It was observed that vanadium oxide or any vanadium compound was not detected and this phenomenon was caused by spectral interferences, because the content of vanadium was very low; to a level where the XRF could not detect the phase, which was likely due to spectral interferences and the low vanadium content. The vanadium concentration was at such a low level that it fell below the detection limit of the XRF spectroscopy. This observation is further supported by the ICP-OES results presented in Table 2, where vanadium exhibited the lowest concentration

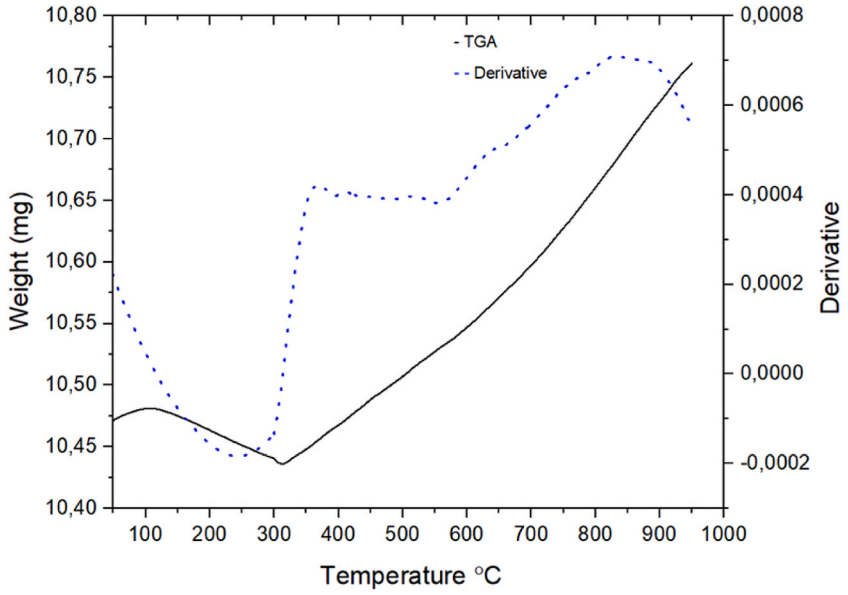

Fig. 5. Thermogravimetric analysis of as-received roast-leach ferrovanadium residue.

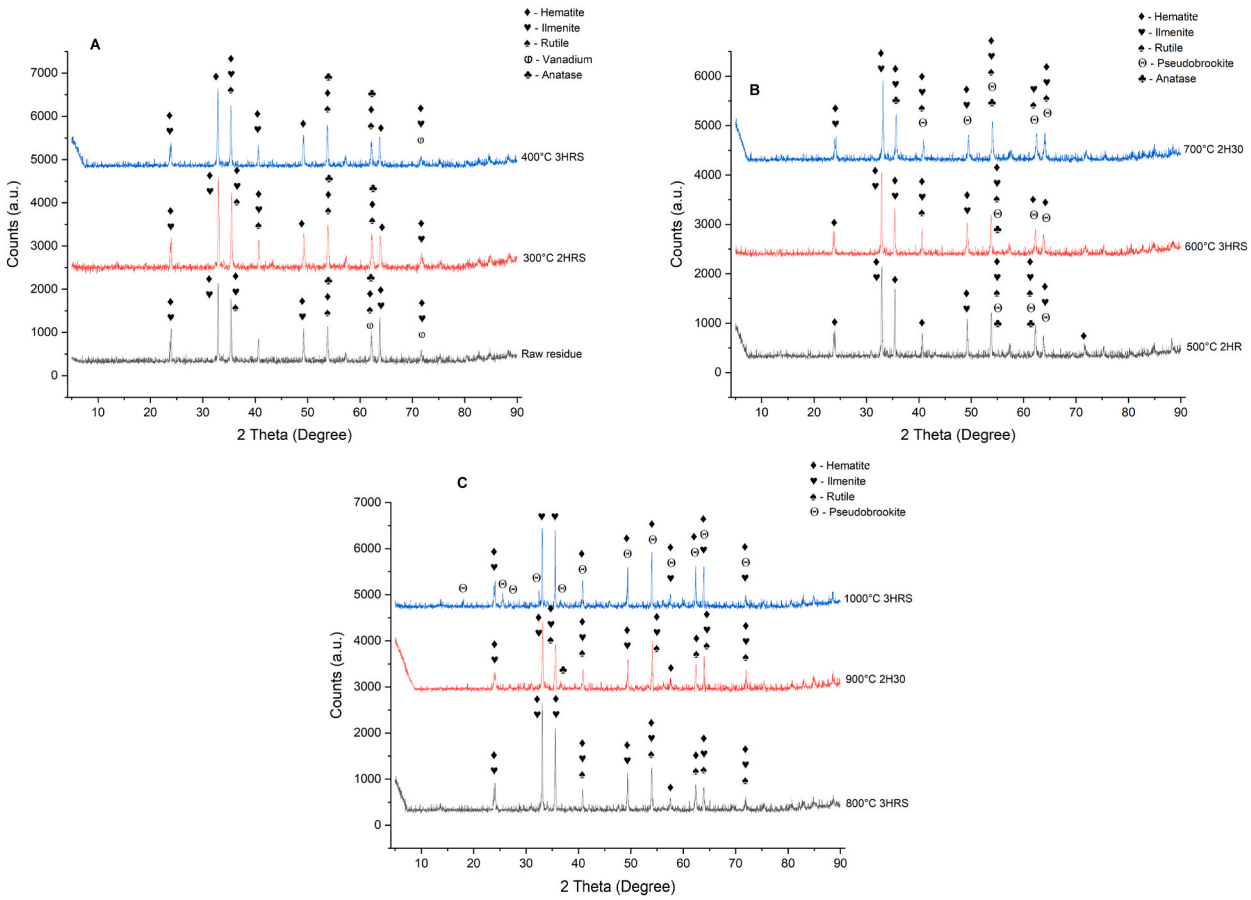

Fig. 6. XRD patterns for the pre-oxidation residue at temperatures ranging from (A) room temperature to 400 °C, (B) 500 °C–700 °C and (C) 800 °C–1000 °C.

Table 3
Mineralogical quantification of the pre-oxidized residue at different temperatures and raw residue determined by XRD analysis.

	Weight (%)								
	1000 °C	900 °C	800 °C	700 °C	600 °C	500 °C	400 °C	300 °C	Raw
Hematite	31.1	42.8	48.7	49.8	49.2	28.7	42.4	42.1	42.9
Rutile		1.5	1.7	1.8	1.7		1.5	1.5	1.5
Ilmenite	31.5	46.2	49.1	48.4	49.0	28.2	43.4	43.3	42.4
Anatase		13.1				8.7	12.7	13.1	13.2
Vanadium	0.3		0.5						
Pseudobrookite	37.2					34.4			

Table 4
Chemical composition of the pre-oxidized roast-leach ferrovanadium residue determined by XRF analysis.

	Components (wt. %)								
	Na_2O	MgO	Al_2O_3	SiO_2	CaO	TiO_2	Cr_2O_3	Fe_2O_3	SO_3
Pre-oxidized slag at 700°C	1.89	0.16	2.15	2.79	0.73	13.66	0.13	76.70	0.76
Pre-oxidized slag at 800°C	1.04	0.19	2.83	2.42	0.69	14.01	0.17	77.52	0.82
Pre-oxidized slag at 900°C	1.66	0.17	2.43	2.95	0.61	13.56	0.14	76.91	0.78

amongst the other elements, *viz*: Fe, Ti, and V. Additionally, Fig. 6 in the XRD analysis, displays ilmenite, as the dominant phase across all particle sizes, providing further confirmation of the low vanadium content within the residue.

3.2.3. SEM analysis of pre-oxidized roast-leach ferrovanadium residue

Figs. 7–10 present the SEM micrographs and EDS data of the raw and the pre-oxidized roast-leach ferrovanadium residue, processed for a duration of 2 h at temperatures of 700 °C, 800 °C, and 900 °C. These specific temperatures and duration were selected based on the XRD analysis, which confirmed the significant formation of hematite and slight increase of rutile at these conditions. The raw residue is depicted in Fig. 7, revealing a rough texture, indicating the fact that the morphology remained unaltered. Additionally, the Energy Dispersive X-ray (EDS) elemental mapping micrograph in Fig. 7, showcases different shades of grey colour and textures, representing various compounds. The dominant light grey colour with a smoother texture, corresponds to ilmenite. In contrast, a blackish or darker shade, less smooth than ilmenite, exhibits high intensities for vanadium, titanium, as well as the presence of impurities, such as alumina (Aℓ) and silica (Si). These impurities are inter-deposited within the ilmenite grains, forming pits. The SEM results depicted in Figs. 8–10, focussed on the pre-oxidized residue, processed for a duration of 2 h at temperatures: 700 °C, 800 °C, and 900 °C, revealing significant changes in morphology. The presence of pores is evident, indicating the fact that these pores did expand during the heating process. This observation aligns with the occurrence of a phase transformation, as confirmed by the XRD results.

Fig. 7 shows the EDS analysis on spectrum 1 of the raw residue. There are many elements in traces, strongly suggesting the fact that the residue contained magnetite and possibly hematite. The presence of Ca, Si, Aℓ, O, means that the raw residue, contained: ilmenite, sphene, plagioclase, quartz, hematite, rutile, and anatase. Fig. 8 shows the EDS analysis on spectrum 1 of the pre-oxidized residue at 700 °C, while Fig. 9, spectrum 2 of pre-oxidized residue at 800 °C and Fig. 10 shows pre-oxidized residue at 900 °C. Carbon was eliminated from the results because the presence of C can be attributed to the double-sided carbon tape, used to stick the samples for SEM analysis. The presence of Fe, Ti and V in all spectra of the EDS analyses, as evidenced in Figs. 7–9 and **10**, confirmed the XRD, and XRF results and the assertion by Geldenhuys [5] that there exist, the opportunities to optimally extract iron, vanadium and titanium by optimising the titanomagnetite slag operating conditions.

3.2.4. ICP-OES analysis of pre-oxidized residue and raw residue

The pre-oxidation process involved heating the slag from 300 °C to 1000 °C, with specific temperatures ranging from 700 °C to 900 °C selected as they represented the optimal conditions for rutile formation. This selection was based on the XRD results presented in Fig. 6, as well as findings from a previous study by Ramakokovhu et al. [29]. At these chosen temperatures (700 °C–900 °C), aqua regia was utilized to digest the slag, enabling the quantification of iron, titanium, and vanadium extraction using the ICP-OES instrumental technique.

Fig. 11 **(A)** illustrates the quantities of iron and titanium, while Fig. 11 (B) shows vanadium extraction for the different residue samples. The highest extraction quantities were observed in the raw residue samples at 69,900.00 mg/L, 5710.00 mg/L and 67.90 mg/L, for Fe, Ti, and V, respectively. Conversely, the lowest extraction for Fe, Ti, and V was observed in the pre-oxidized residue samples compared to the raw residue. This disparity was attributed to the formation of non-amenable phases, such as pseudobrookite, which began to emerge at 500 °C and became more dominant above 900 °C, as observed in the XRD analysis (section 3.2.1). This observation suggests that the conventional pre-oxidation of complex phases into simpler leachable phases may not be suitable for the roast-leach ferrovanadium residue, as evidenced by the ICP results showing higher recovery of Fe, Ti, and V in the raw residue rather than in the pre-oxidized residue.

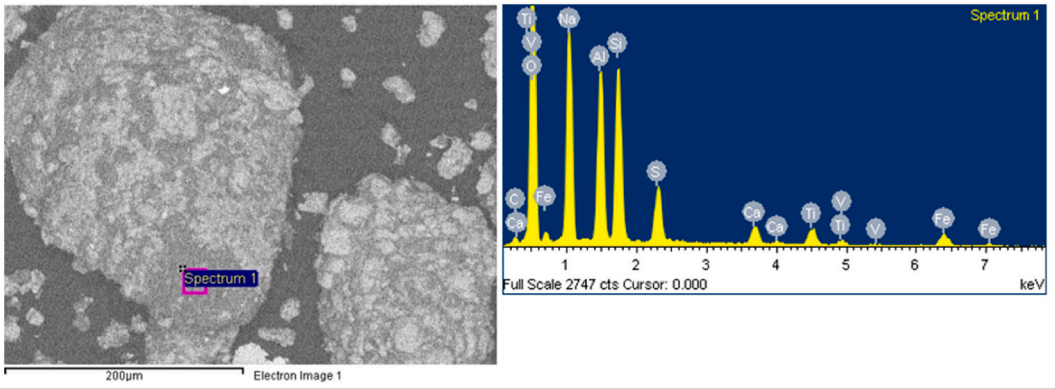

Element	C	O	Na	Mg	Al	Si	S	Ca	Ti	V	Fe	Total
Weight%	2.89	49.13	14.43	0.06	9.12	10.47	4.09	1.97	2.75	0.52	4.58	100
Atomic%	4.83	61.69	12.6	0.05	6.79	7.48	2.56	0.99	1.15	0.2	1.65	100

Fig. 7. SEM Micrograph and EDS of the raw roast-leach ferrovanadium residue.

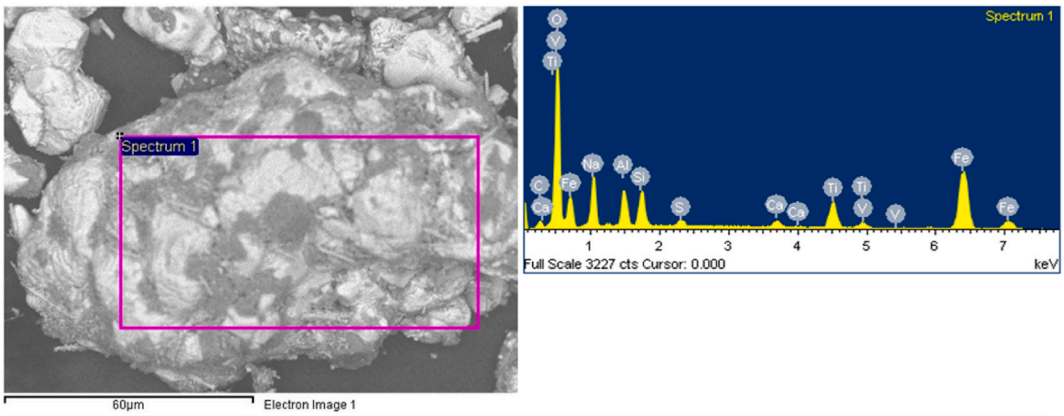

Element	C	O	Na	Mg	Al	Si	S	Ca	Ti	V	Mn	Fe	Total
Weight%	3.72	35.75	7.57	0.19	3.55	3.51	0.75	0.99	6.44	0.56	0.28	36.69	100
Atomic%	7.76	55.95	8.25	0.19	3.29	3.13	0.58	0.62	3.37	0.28	0.13	16.45	100

Fig. 8. SEM Micrograph and EDS of the pre-oxidized residue at 700 °C for 2 h.

4. Conclusion

This study presents the characterization and the pre-oxidation findings of the roast-leach ferrovanadium residue, including the sequence of phase transformations during the pre-oxidation process. The extraction potential of the raw residue versus the pre-oxidized residue was also evaluated. PSD analysis showed a P80 of 200 µm after milling. The XRF analysis revealed the presence in the residue, for hematite (75.55%), titanium dioxide (12.79%), silica (3.03%), and alumina (2.62%).

XRD analysis revealed the presence of ilmenite ($FeTiO_3$) and vanadium dioxide (VO_2) phases in the as-received samples, with Thermogravimetric analysis highlighting critical phase transformation temperatures at 350 °C and 816 °C. This data facilitated the precise targeting of optimal oxidation temperatures, crucial for obtaining desired phases prior to subsequent leaching processes. Furthermore, consistent results from XRD, XRF, and SEM analyses confirmed the formation of new phases such as hematite, rutile, anatase, and pseudobrookite. Notably, the dominance of pseudobrookite phases at temperatures exceeding 900 °C was evident from XRD analysis of the pre-oxidized residue.

Despite the promising phase transformations observed, uncertainties arose about the feasibility of pre-oxidizing the complex roast-leach ferrovanadium residue to leachable phases. Analysis using ICP-OES revealed low extraction of Fe, V, and Ti quantities in the pre-oxidized residue compared to the raw residue. This is attributed to the formation of non-amenable phases, particularly pseudobrookite, which emerged at 500 °C and became more dominant above 900 °C.

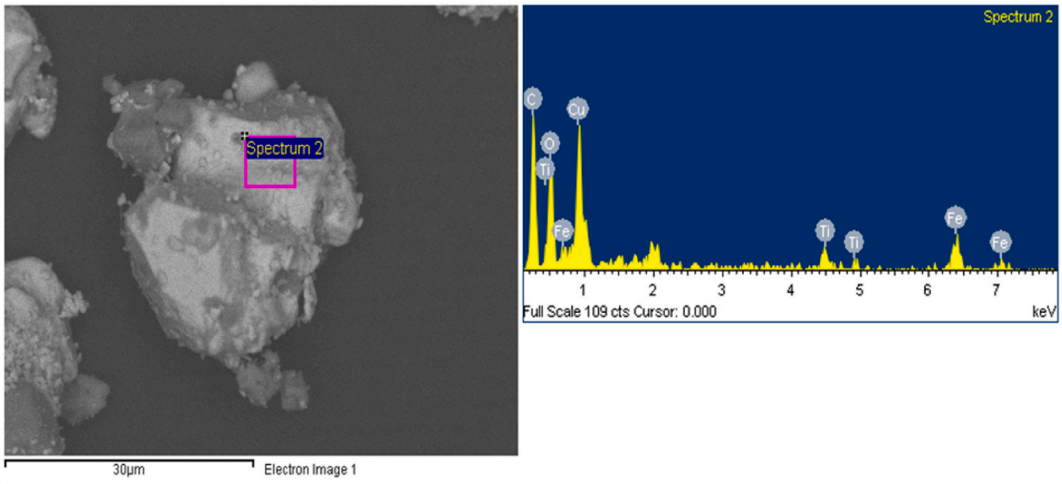

Element	C	O	Al	Ti	Fe	Cu	Ir	Total
Weight%	38.66	22.78	0.52	2.79	11.96	19.52	3.77	100
Atomic%	61.18	27.07	0.37	1.11	4.07	5.84	0.37	100

Fig. 9. SEM Micrograph and EDS of the pre-oxidized residue at 800 °C for 2 h.

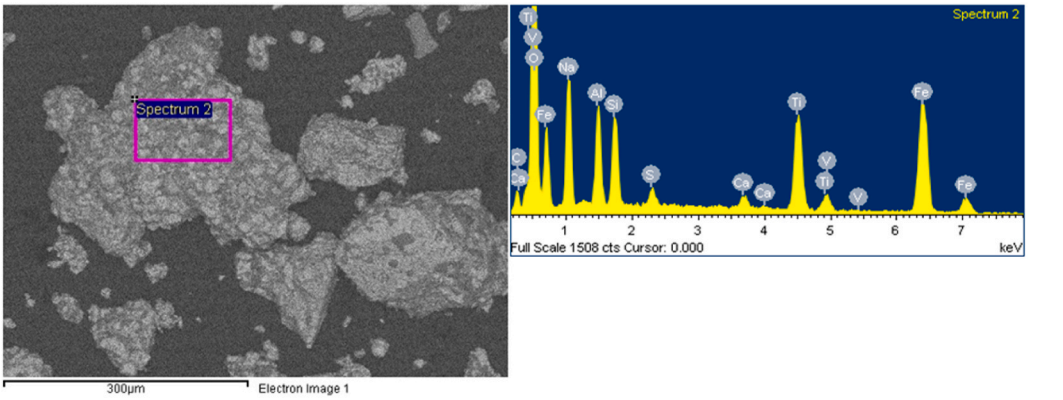

Element	C	O	Na	Mg	Al	Si	S	Cl	Ca	Ti	V	Mn	Fe	Total
Weight%	3.8	41.27	7.57	0.09	3.74	3.48	0.77	0.06	0.76	9.8	0.51	0.08	28.06	100
Atomic%	7.44	60.63	7.74	0.09	3.26	2.91	0.56	0.04	0.45	4.81	0.24	0.04	11.81	100

Fig. 10. SEM Micrograph and EDS of the pre-oxidized residue at 900 °C for 2 h.

Data availability statement

The data that support the findings of this study are available from the corresponding author, Ms. M. Nevondo (mbavhanevondo@gmail.com), upon reasonable request.

CRediT authorship contribution statement

M. Nevondo: Writing - original draft, Methodology, Investigation, Review & editing, Visualization, Validation. **L. Koech:** Writing - review & editing, Validation. **O.O. Ola-omole:** Writing - review & editing, Supervision. **M. M Ramakokovhu:** Conceptualization, Visualization, Supervision, Review & editing. **M. L. Teffo:** Review & editing, Supervision. **R. Sadiku:** Review & editing.

Declaration of competing interest

The authors declare that they have no known competing financial interests or personal relationships that could have appeared to influence the work reported in this paper.

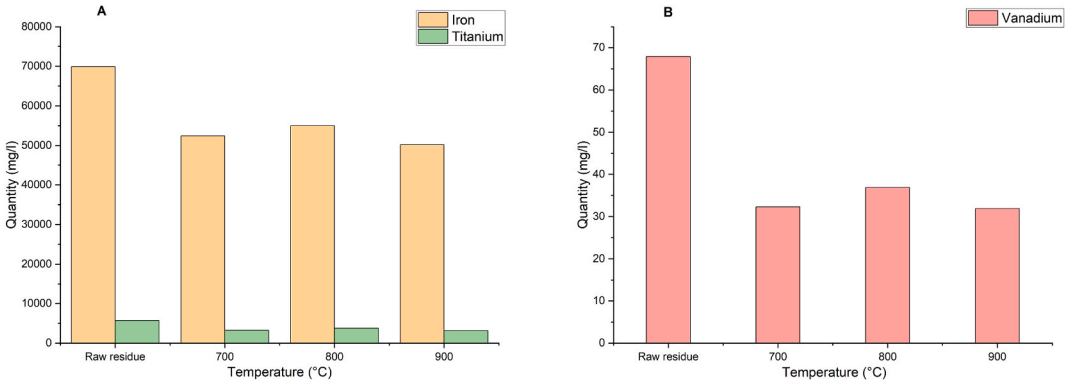

Fig. 11. Extracted quantities of (A) Fe, Ti and (B) V under varying pre-oxidation temperatures.

References

[1] C. Brough, R.J. Bowell, J. Larkin, The Geology of Vanadium Deposits, an Introduction to Vanadium, 2019, pp. 87–117.
[2] Q. Yuan, O. Namur, L.A. Fischer, R.J. Roberts, X. Lü, B. Charlier, Pulses of plagioclase-laden magmas and stratigraphic evolution in the Upper Zone of the Bushveld complex, South Africa, J. Petrol. 58 (2017) 1619–1643.
[3] R. Gilligan, A.N. Nikoloski, The extraction of vanadium from titanomagnetites and other sources, Miner. Eng. 146 (2020) 106106.
[4] C. Lv, S. Bai, Upgrading of Raw Vanadium Titanomagnetite Concentrate, vol. 119, Journal of the Southern African Institute of Mining and Metallurgy, 2019, pp. 957–961.
[5] I.J. Geldenhuys, Feasibility of Fluxless Smelting of Titaniferous Magnetite Ore in a Pilot-Plant Open-Arc Dc Furnace, Stellenbosch University, Stellenbosch, 2020. PhD Thesis, https://scholar.sun.ac.za/handle/10019.1/108177. (Accessed 20 January 2024).
[6] Y. Dong, Y. Zhao, H. Lin, C. Liu, Effect of physical and chemical properties of vanadium slag from stone coal on the form of vanadium, Environ. Sci. Pollut. Res. 26 (2019) 33004–33013, https://doi.org/10.1007/s11356-019-06381-7.
[7] J.-H. Huang, F. Huang, L. Evans, S. Glasauer, Vanadium: Global (bio) geochemistry, Chem. Geol. 417 (2015) 68–89.
[8] G. Wang, M.-M. Lin, J. Diao, H.-Y. Li, B. Xie, G. Li, Novel strategy for green comprehensive utilization of vanadium slag with high-content chromium, ACS Sustainable Chem. Eng. 7 (2019) 18133–18141, https://doi.org/10.1021/acssuschemeng.9b05226.
[9] J. Lee, E. Kim, K.W. Chung, R. Kim, H.-S. Jeon, A review on the metallurgical recycling of vanadium from slags: towards a sustainable vanadium production, J. Mater. Res. Technol. 12 (2021) 343–364.
[10] A.M. Herbst, Vanadium extraction by roast-leach method with tailings from mustavaara (Finland) and titania (Norway), and Kiruna magnetite (Sweden), New Mexico Institute of Mining and Technology (2020). https://search.proquest.com/openview/941ed98c57923714fd47e73b71a7bbb1/1?pq-origsite=gscholar&cbl=51922&diss=y. (Accessed 20 January 2024).
[11] M. Sitefane, M. Masipa, P. Maphutha, X.C. Goso, The effect of CaO to MgO ratio on the smelting characteristics of vanadium-bearing titaniferous magnetite, in: Proceedings of the 3rd Young Professional Conference Innovation Hub, Pretoria, The Southern African Institute of Mining and Metallurgy, 2017, pp. 467–480. https://www.pyrometallurgy.co.za/Mintek/Files/2017Sitefane.pdf. (Accessed 20 January 2024).
[12] M. Ochsenkuehn-Petropoulou, L.-A. Tsakanika, T. Lymperopoulou, K.-M. Ochsenkuehn, K. Hatzilyberis, P. Georgiou, C. Stergiopoulos, O. Serifi, F. Tsopelas, Efficiency of sulfuric acid on selective scandium leachability from bauxite residue, Metals 8 (2018) 915.
[13] S.Y. Chen, M.S. Chu, A New Process for the Recovery of Iron, Vanadium, and Titanium from Vanadium Titanomagnetite, vol. 114, Journal of the Southern African Institute of Mining and Metallurgy, 2014, pp. 481–488.
[14] X.C. Goso, Phase Equilibria Studies and Beneficiation of Titaniferous Slags, University of Cape Town, 2019.
[15] G. Ye, Recovery of Vanadium from LD Slag, a State of the Art Report: Part 1 - Facts and Metallurgy of Vanadium, Jernkontoret, 2006.
[16] S. Nkosi, P. Dire, N. Nyambeni, X.C. Goso, A comparative study of vanadium recovery from titaniferous magnetite using salt, sulphate, and soda ash roast-leach processes, in: 3rd Young Professionals Conference, 2017, pp. 191–200. https://www.pyro.co.za/Mintek/Files/2017Nkosi.pdf. (Accessed 20 January 2024).
[17] X.C. Goso, H. Lagendijk, M. Erwee, G. Khosa, Indicative vanadium deportment in the processing of titaniferous magnetite by the roast–leach and electric furnace smelting processes, in: Hydrometallurgy Conference, 2016. https://www.pyro.co.za/Mintek/Files/2016Goso2.pdf. (Accessed 20 January 2024).
[18] X. Wang, J. Xiang, J. Ling, Q. Huang, X. Lv, Comprehensive utilization of vanadium extraction tailings: a brief review, in: X. Chen, Y. Zhong, L. Zhang, J. A. Howarter, A.A. Baba, C. Wang, Z. Sun, M. Zhang, E. Olivetti, A. Luo, A. Powell (Eds.), Energy Technology 2020: Recycling, Carbon Dioxide Management, and Other Technologies, Springer International Publishing, Cham, 2020, pp. 327–334, https://doi.org/10.1007/978-3-030-36830-2_31.
[19] L. Dong, X. Tong, X. Li, J. Zhou, S. Wang, B. Liu, Some developments and new insights of environmental problems and deep mining strategy for cleaner production in mines, J. Clean. Prod. 210 (2019) 1562–1578.
[20] M.M. Ramakokovhu, T. Mojisola, R.K.K. Mbaya, P.A. Olubambi, B.D. Baloyi, L. Malaka, An electrochemical study and thermodynamic quantification of pre-oxidized ilmenite metastable phases, in: Proceedings of the 11th International Heavy Minerals Conference, Western Cape, South Africa, 2019, pp. 5–6. (Accessed 20 January 2024).
[21] M.H. Rodriguez, G.D. Rosales, E.G. Pinna, F.M. Tunez, N. Toro, Extraction of titanium from low-grade ore with different leaching agents in autoclave, Metals 10 (2020) 497.
[22] S. Samal, B.K. Mohapatra, P.S. Mukherjee, S.K. Chatterjee, Integrated XRD, EPMA and XRF study of ilmenite and titania slag used in pigment production, J. Alloys Compd. 474 (2009) 484–489.
[23] D. Michaud, Table of bond work index by minerals, mineral processing & metallurgy. https://www.911metallurgist.com/blog/table-of-bond-work-index-by-minerals, 2015. (Accessed 20 January 2024).
[24] H. Mkurazhizha, The effects of ore blending on comminution behaviour and product quality in a grinding circuit-Svappavaara (LKAB) Case Study. https://www.diva-portal.org/smash/get/diva2:1239628/FULLTEXT01.pdf, 2018. (Accessed 20 January 2024).
[25] L. Palliyaguru, U.S. Kulathunga, L.I. Jayarathna, C.D. Jayaweera, P.M. Jayaweera, A simple and novel synthetic route to prepare anatase TiO2 nanopowders from natural ilmenite via the H3PO4/NH3 process, Int. J. Miner. Metall. Mater. 27 (2020) 846–855, https://doi.org/10.1007/s12613-020-2030-3.
[26] K. Wu, Y. Wang, X. Wang, S. Wang, B. Liu, Y. Zhang, H. Du, Co-extraction of vanadium and chromium from high chromium containing vanadium slag by low-pressure liquid phase oxidation method, J. Clean. Prod. 203 (2018) 873–884.
[27] Y. Zhang, L. Yi, L. Wang, D. Chen, W. Wang, Y. Liu, H. Zhao, T. Qi, A novel process for the recovery of iron, titanium, and vanadium from vanadium-bearing titanomagnetite: sodium modification–direct reduction coupled process, Int. J. Miner. Metall. Mater. 24 (2017) 504–511, https://doi.org/10.1007/s12613-017-1431-4.
[28] S.E. Haggerty, Oxide textures-a mini-atlas, Oxide Minerals: Petrologic and Magnetic Significance 25 (1991) 129–219.

[29] M.M. Ramakokovhu, P.A. Olubambi, R.K.K. Mbaya, T. Mojisola, M.L. Teffo, Mineralogical and leaching characteristics of altered ilmenite beach placer sands, Minerals 10 (2020) 1022.
[30] M.P. Maphutha, M. Ramaili, M.B. Sitefane, X.C. Goso, The effect of magnesia and alumina crucible wear on the smelting characteristics of titaniferous magnetite, Journal of the Southern African Institute of Mining and Metallurgy 117 (2017) 649–655.
[31] X. Fu, Y. Wang, F. Wei, Phase transitions and reaction mechanism of ilmenite oxidation, Metall. Mater. Trans. A 41 (2010) 1338–1348, https://doi.org/10.1007/s11661-010-0173-y.
[32] M. Guéguin, F. Cardarelli, Chemistry and mineralogy of titania-rick slags. Part 1-Hemo-Ilmenite, sulphate, and upgraded titania slags, Miner. Process. Extr. Metall. Rev. 28 (2007) 1–58, https://doi.org/10.1080/08827500600564242.